





## Reducing computational complexity in fingerprint matching

Mubeen SABIR<sup>1,\*</sup>, Tariq M. KHAN<sup>1</sup>, Munazza ARSHAD<sup>2</sup>, Sana MUNAWAR<sup>3</sup>

<sup>1</sup>Electrical and Computer Engineering Department, COMSATS University, Islamabad, Pakistan

<sup>2</sup>ARDIC, Heavy Industries Taxila, Pakistan

<sup>3</sup>Software Engineering Department, University of Engineering and Technology, Taxila, Pakistan

Received: 15.07.2019

Accepted/Published Online: 25.02.2020

Final Version: 25.09.2020

**Abstract:** The performance of cross-correlation functions can decrease computational complexity under optimal fingerprint feature selection. In this paper, a technique is proposed to perform alignment of fingerprints followed by their matching in fewer computations. Minutiae points are extracted and alignment is performed on the basis of their spatial locations and orientation fields. Unlike traditional cross-correlation based matching algorithms, ridges are not included in the matching process to avoid redundant computations. However, optimal cross-correlation is chosen by correlating feature vectors accompanying  $x$ - $y$  locations of minutiae points and their aligned orientation fields. As a result, matching time is significantly reduced with much improved accuracy.

**Key words:** Biometrics, cross-correlation, minutiae points, filtering, matching

### 1. Introduction

Patterns of immutable friction ridges and valleys forming fingerprints that have been extensively used for identification in numerous fields may be located on the exterior of one's fingertip that have been extensively used for identification in numerous fields. Due to increased cybercrimes and security frauds, uses of biometric-based access control technology is growing vigorously [1]. There are different biometric traits such as gait, iris, face, speech, etc. However, as far as authenticity, uniqueness, and reliability are concerned, the fingerprint is most widely used biometric trait in almost all fields for instance institutions, banks, border security, smartphones, laptops and cash machines [2].

To provide fingerprint-based biometric authentication, different algorithms have been proposed, mainly minutiae-based, pattern-based, correlation-based, etc. However, all rely on feature extraction of different types such as core point, delta, minutiae points, pores, and ridge valley structures [3].

Smartphones and related devices acquire very less area of finger for recognition through scanner. In this regard, a secure algorithm is developed for fingerprint authentication using the cross correlation-based technique as well as entropy is obtained for the associated region. The captured region is divided into blocks, different weights are assigned to them to extract features and score is calculated [4]. Normalized cross-correlation is performed between the input image and template image by first finding the region of interest near the core point on the fingerprint image. A couple of translations are applied and correlation is calculated on the selected region to reduce computations and finally score is generated [5]. A multilayer feed-forward (FF) artificial neural network (backpropagation) is created. Superimposition of features undergo training and testing steps to facilitate the matching. In this way, improved accuracy is found [6]. Authentication and identification for

\*Correspondence: mubeensabir@comsats.edu.pk

fingerprints over the large datasets require larger memory. A flexible scoring technique is proposed through which decomposition of matching and corresponding generation of score is performed to avoid larger size structures for its accommodation [7]. Partial fingerprint matching is performed by acquiring features involving ridge-shapes as well as minutiae points. Devices (such as mobile phones and laptops) require only minute scan accompanying insufficient region that may not be enough for provision of authentication using traditional matching techniques. Therefore, structures of the ridges' shapes as convex or concave are obtained to ease the matching steps [8]. Fingerprint-based unlocking of smartphones demand faster algorithms. Therefore, matching using binary descriptors relying on phase correlations is carried out and required operation is achieved comparatively in less time lag [9]. Orientation field is extracted from ridge valley patterns followed by features (minutiae points). Relations among minutiae points are developed and decision of matching is obtained from similarity function [10]. To introduce uniqueness in the matching process of fingerprints, two descriptors are created for each minutia points followed by a seventeen-dimensional feature vector and then the greedy matching algorithm is used for classification [11]. Matching of fingerprint images is performed based on minutiae points by dividing into two blocks. First extract features and second execute matching on the basis of extracted features and their angles from the reference point [12].

Reduction of computational cost and improvement in accuracy are key aspects of a system. In this paper, a cross-correlation ( $CC$ ) technique is employed to achieve matching of fingerprints in a less time lag with improved accuracy. Section II discusses the enhancement and feature extraction. Section III covers the traditional cross correlation-based matching; whereas its drawbacks and proposed cross correlation-based matching is provided in sections IV and V, respectively. Section VI provide the details of performance evaluation parameters. In section VII, results and their discussion are provided followed by the conclusion in section VIII.

## 2. Enhancement of fingerprints

Before going into the matching stage, removal of noise and unwanted contents is compulsory. Therefore, to carry out enhancement, first, normalization is required to be performed to get predefined mean and variance over the fingerprint image. Mean and variance may be calculated as:

$$\mu(I) = \frac{1}{R \times C} \sum_{i=0}^{R-1} \sum_{j=0}^{C-1} I(i, j), \quad (1)$$

$$\nu(I) = \frac{1}{R \times C} \sum_{i=0}^{R-1} \sum_{j=0}^{C-1} (I(i, j) - \mu(I))^2, \quad (2)$$

where  $I$  is the input image,  $(i, j)$  shows location of pixel at  $i^{th}$  row and  $j^{th}$  column on  $I$ ,  $(R \times C)$  shows size,  $\mu$  mean and  $\nu$  variance of  $I$ , respectively. Now, normalization may be applied to reduce the abrupt changes across the ridges as follows [13]:

$$G(i, j) = \begin{cases} \mu_o + \sqrt{\frac{\nu_o(I(i,j)) - \mu^2}{\nu}}, & \text{if } I(i, j) > \mu \\ \mu_o - \sqrt{\frac{\nu_o(I(i,j)) - \mu^2}{\nu}}, & \text{elsewhere} \end{cases} \quad (3)$$

where  $G$  is the normalized image,  $\mu_o$  and  $\nu_o$  are desired mean and variance, respectively. Normalization does not change the clarity of the image but it facilitates subsequent steps such as estimation of orientation, frequency of ridges and filtering process.

The orientation of friction-ridges lead toward the uniqueness of fingerprints and has a vital role in filtering and eventually in the authentication of a human being. For this,  $G$  is required to be converted into blocks of size ( $w = 16$ ) and gradient is obtained as given in following.

$$V_x(i, j) = \sum_{u=i-w/2}^{i+w/2} \sum_{v=j-w/2}^{j+w/2} 2\partial_x(u, v)\partial_y(u, v), \tag{4}$$

$$V_y(i, j) = \sum_{u=i-w/2}^{i+w/2} \sum_{v=j-w/2}^{j+w/2} (\partial_x^2(u, v) - \partial_{xy}^2(u, v)), \tag{5}$$

$$\theta(i, j) = \frac{1}{2} \tan^{-1} \left( \frac{V_y(i, j)}{V_x(i, j)} \right), \tag{6}$$

where  $\theta$  is estimate of orientation field centered at pixel  $(i, j)$ . However, the presence of noise degrades  $I$  and destroys ridge valley structures, the deviancy from estimated  $\theta$  may be corrected by applying lowpass filtering. To apply lowpass filtering, the estimated orientation field is first converted into continuous field as given in following.

$$\Phi_x(i, j) = \cos(2\theta(i, j)), \tag{7}$$

$$\Phi_y(i, j) = \sin(2\theta(i, j)), \tag{8}$$

where  $\Phi_x$  and  $\Phi_y$  are the components of the vector field in horizontal and vertical directions. Now, lowpass filtering may be applied to get smoothed orientation field [13].

$$\Phi'_x(i, j) = \sum_{u=-w_\Phi/2}^{w_\Phi/2} \sum_{v=-w_\Phi/2}^{w_\Phi/2} W(u, v)\Phi_x(i - uw, j - vw), \tag{9}$$

$$\Phi'_y(i, j) = \sum_{u=-w_\Phi/2}^{w_\Phi/2} \sum_{v=-w_\Phi/2}^{w_\Phi/2} W(u, v)\Phi_y(i - uw, j - vw), \tag{10}$$

where  $W(\cdot)$  is the lowpass filter with its size ( $w_\Phi = 5$ ), and smoothed orientation  $\vartheta$  can be calculated as:

$$\vartheta(i, j) = \frac{1}{2} \tan^{-1} \left( \frac{\Phi'_y(i, j)}{\Phi'_x(i, j)} \right). \tag{11}$$

Frequency of ridge valley patterns is another unique feature of fingerprint image that eases filtering process. Varying patterns of ridges and valleys can be modeled as sinusoidal shaped-wave normal to the orientation. For this, image is divided into blocks of size ( $w = 16$ ) and oriented-window having size of  $(l \times w)$  is created with  $(l = 32)$  and x-signature ( $X$ ) is calculated there. If singular points do not appear in oriented-window,  $X$  produces discrete sinusoidal shaped-wave having the same frequency as that of the ridges and furrows in the oriented-window [13].

$$X[k] = \frac{1}{w} \sum_{d=0}^{w-1} G(u, v), k = 0, 1, 2, \dots, l - 1 \tag{12}$$

$$u = i + \left(d - \frac{w}{2}\right) \cos(\vartheta(i, j)) + \left(k - \frac{l}{2}\right) \sin(\vartheta(i, j)), \quad (13)$$

$$v = j + \left(d - \frac{w}{2}\right) \sin(\vartheta(i, j)) + \left(\frac{l}{2} - w\right) \cos(\vartheta(i, j)), \quad (14)$$

Patterns of ridges and valleys accompanying unique information regarding orientation and frequency can be benefited to remove noise from fingerprint. Since sinusoidal shaped-wave varies slowly with local orientation, Gabor filter in bandpass mode tuned to corresponding frequency and orientation may be used to preserve actual patterns.

$$h(x, y : \phi, f) = \exp \left\{ -\frac{1}{2} \left[ \frac{(x \cos(\phi))^2}{\delta_x^2} + \frac{(y \sin(\phi))^2}{\delta_y^2} \right] \right\} \cos(2\pi f x \cos(\phi)), \quad (15)$$

where  $h$  is an impulse response of even symmetric Gabor filter,  $\phi$  shows the corresponding orientation of the Gabor filter,  $f$  shows the frequency of the sinusoidal wave,  $\delta_x$  and  $\delta_y$  denote the standard deviations of the Gaussian envelop along horizontal and vertical, respectively [14]. The input image and its enhanced version are shown in Figures 1a and 1b.

### 3. Matching using $CC$

After performing enhancement, images undergo matching stages, so that degree of similarity between template and input images may be figured out. For this, most widely used method i.e. cross-correlation based matching technique is employed [1].

Let,  $T$  be the template image and  $I$  be the input image, the degree of diversity between them may be assessed from their squared difference ( $S_D$ ).

$$S_D(T, I) = \|T\|^2 + \|I\|^2 - 2T^T I, \quad (16)$$

where  $(.)^T$  in superscript shows transpose. However, the third term in (16) corresponds to their cross correlation ( $CC$ ) or the degree of similarity as given in (17).

$$CC(T, I) = T^T I, \quad (17)$$

If  $T$  and  $I$  are samples of each other then  $CC$  would be maximum. However, on the other hand,  $S_D$  would be minimized. Since fingers vary in placement during their acquisition and thereby patterns of ridges and valleys arise differently hence information changes [15]. Therefore, the calculation of a simple correlation does not provide the maximum degree of similarity. It may be increased optimally, under suitable translations and rotations followed by correlation on each step.

$$S_M(T, I) = \max_{\Delta x, \Delta y, \Delta \theta} CC(T, (I)^{\Delta x, \Delta y, \Delta \theta}), \quad (18)$$

where  $\Delta x$  and  $\Delta y$  are translations in horizontal and vertical directions whereas,  $\Delta \theta$  shows rotations in clockwise or anticlockwise around the origin of the fingerprint image.

**4. Limitations of CC**

Implementation of (18) leads poorly toward perfect matching of fingerprints because neither translations nor rotations are well determined. It does not provide any estimation of  $\Delta x$ ,  $\Delta y$  and  $\Delta\theta$ . It executes redundant translations and rotations. Insufficient translations cause mismatched overlapping that brings dissimilarity and decreases  $S_M$ . Then execution of rotations upon them produce misalignment of ridges, ridge endings as well as ridge bifurcations. Thereby, it becomes computationally heavy, redundant and compromise the accuracy.

**5. Proposed matching algorithm**

To avoid useless translations, rotations and to decrease computations, features (minutiae points) may be acquired followed by their orientation fields to estimate their proper locations; so that purpose of alignment may be handled, accordingly. The enhanced image may be binarized to perform thinning so that ridges may be squeezed to a single pixel and minutiae extraction stage could be eased as shown in Figure 1c.

For the extraction of minutiae points, thinned image ( $T_d$ ) is divided into blocks of size  $(3 \times 3)$  and zero to one crossings are noted in eight adjacent neighbors [16].

$$Z_c = \left(\frac{1}{2}\right) \sum_{i=1}^8 |B_i - B_{i+1}|, \tag{19}$$

where  $Z_c$  shows the numbers of zero to one crossings on  $B_i$  pixels over thinned image as illustrated in Figure 2.



Figure 1: (a): Input image, (b): Enhanced input image, (c): Thinned image.

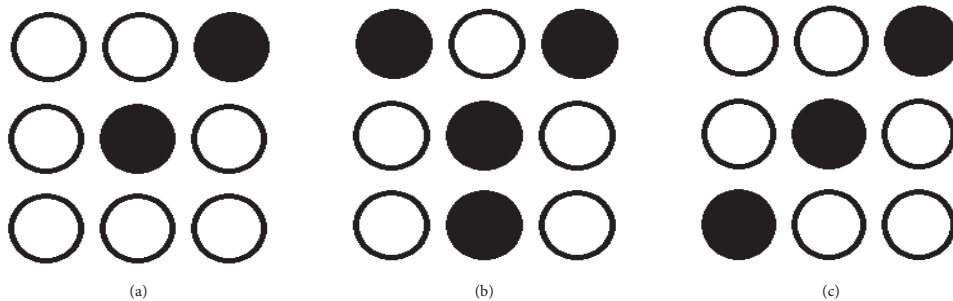


Figure 2: Three by three scan of  $T_d$  for the extraction of minutiae points (a): Ridge ending, (b): Ridge bifurcation, (c): Continued ridge.

If  $Z_c$  comes out to be “1” then it would be considered as ridge ending, for  $Z_c$  equal to “2” it would be neither ridge ending nor ridge bifurcation and if its value is “3” then that would be the ridge bifurcation. The extracted minutiae points are shown in Figure 3a with small circles.

$$Z_c = \begin{cases} 1, & \text{ridge ending} \\ 2, & \text{continued ridge} \\ 3, & \text{ridge bifurcation} \end{cases} \quad (20)$$

After the extraction of minutiae points, the images may be aligned based on their minutiae locations and orientation fields. Let triplet  $M_i$ , accompanying  $x$ - $y$  and orientation  $\vartheta_i$  related information of all minutiae points corresponding to  $T$  and triplet  $M_j$  having same information regarding  $I$  as given in following.

For template image:

$$M_i = x_i, y_i, \vartheta_i \text{ and } i = 1, 2, 3, , m$$

For input image:

$$M_j = x_j, y_j, \vartheta_j \text{ and } j = 1, 2, 3, , n$$

where  $m$  and  $n$  are numbers of minutiae points in  $T$  and  $I$ , respectively [17]. For alignment, let minutiae points from  $M_j$  undergo a translation and rotation according to minutiae points of  $M_i$ .

$$\begin{matrix} \text{map} \\ \Delta x, \Delta y, \Delta \theta \end{matrix} (M_j = \{x_j, y_j, \vartheta_j\}) = M'_j = \{x'_j, y'_j, \Delta \vartheta\} \quad (21)$$

$$\begin{bmatrix} x'_j \\ y'_j \end{bmatrix} = \begin{bmatrix} \cos(\vartheta) & -\sin(\vartheta) \\ \sin(\vartheta) & \cos(\vartheta) \end{bmatrix} \begin{bmatrix} x_j \\ y_j \end{bmatrix} + \begin{bmatrix} \Delta x \\ \Delta y \end{bmatrix}, \quad (22)$$

where  $\Delta x$  is the difference between particular minutia from  $M_i$  and  $M_j$  in  $x$  direction,  $\Delta y$  is the difference between particular minutia from  $M_i$  and  $M_j$  in  $y$  direction; similarly,  $\Delta \vartheta$  is their directional difference.  $M'_j$  shows the resultant transformed triplet by means of translations and rotations according to  $M_i$ .

$$\Delta x = x_i - x_j$$

$$\Delta y = y_i - y_j$$

$$\Delta \vartheta = \begin{cases} \vartheta_i - \vartheta_j & \text{if } (\vartheta_i - \vartheta_j) \geq 0 \\ (\vartheta_i - \vartheta_j) + 180 & \text{if } (\vartheta_i - \vartheta_j) < 0 \end{cases} \quad (23)$$

In order to maximize the similarity between  $T$  and  $I$  optimally, the  $CC$  may be obtained for their extracted triplets.

$$S_O(T, I) = \max\{CC(M_{i_o}(x_{i_o}, y_{i_o}, \vartheta_{i_o}), M'_{j_o}(x'_{j_o}, y'_{j_o}, \Delta \vartheta))\}, \quad (24)$$

where

$$i_o = 1, 2, 3, , \min(m, n)$$

$$j_o = 1, 2, 3, , \min(m, n)$$

In this way optimal similarity  $S_O$  may be obtained in less number of computations as well as in less duration. Overall methodology is shown in flow chart as given in Figure 3b.

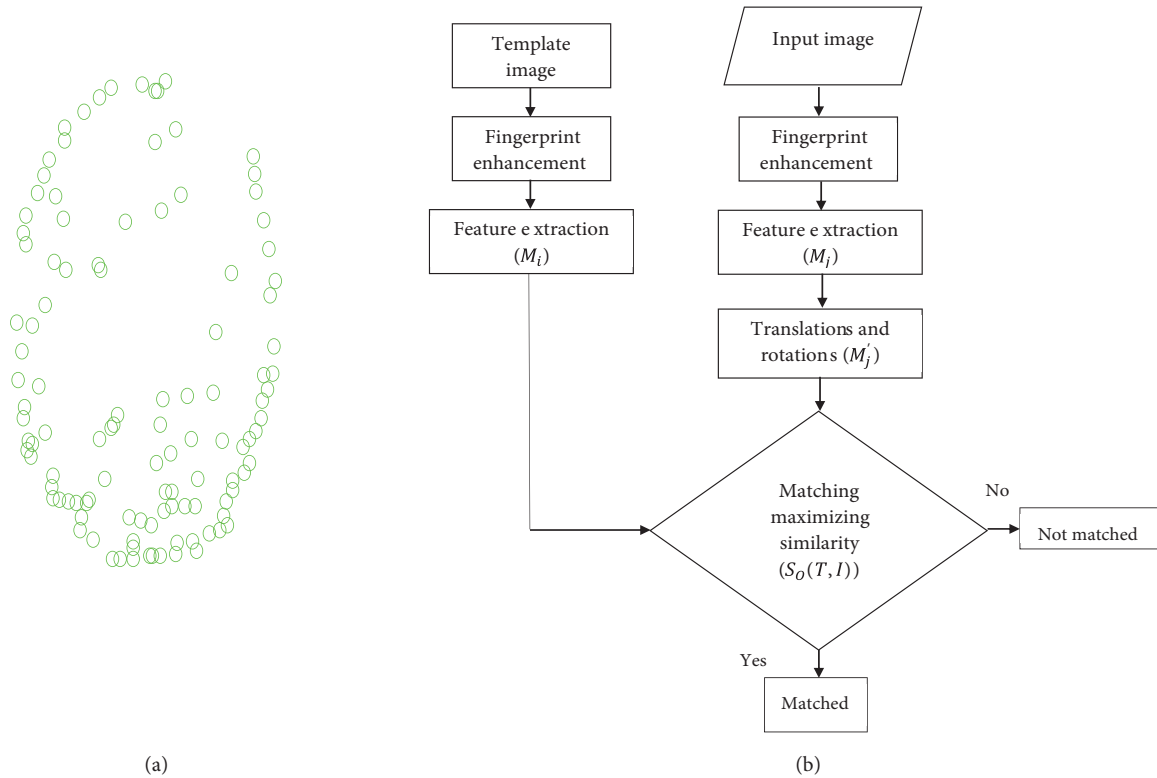


Figure 3: (a): Minutiae points, (b): Flow chart.

**6. Performance evaluation**

In order to evaluate the performance of *CC* and proposed method triplet based cross correlation (TBCC), different parameters such as false nonmatch rate (*FNMR*), false match rate (*FMR*), sensitivity (*S*), specificity (*P*) and accuracy (*A*) are used for evaluation [18].

*FNMR* and *FMR* both give information about an error while performing genuine and imposter matching, respectively. The point where they meet is called equal error rate (EER). Mathematically they can be described as follows:

$$FNMR(t) = \frac{card\{G_s | G_s < t\}}{G_a}, \tag{25}$$

$$FMR(t) = \frac{card\{I_s | I_s > t\}}{I_a}, \tag{26}$$

where *card{.}* gives the cardinality, *G<sub>s</sub>* is genuine matching score under genuine matching attempts (*G<sub>a</sub>*), *t* is threshold and *I<sub>s</sub>* is imposter score under imposter matching attempts *I<sub>a</sub>*. The statistical parameters depend upon true positive (*TP*), true negative (*TN*), false positive (*FP*) and false negative (*FN*) as given in following [19].

$$S = \frac{TP}{TP + FN}, \tag{27}$$

$$P = \frac{TN}{TN + FP}, \tag{28}$$

$$A = \frac{TP + TN}{TP + FP + FN + TN}. \quad (29)$$

## 7. Results and discussion

### 7.1. Data bases

For experiments different databases such as FVC2000DB1A<sup>1</sup>, FVC2002DB1A<sup>2</sup>, FVC2006DB1A<sup>3</sup> [20] and LivDet2009<sup>4</sup> [21] fingerprint databases are used. All these databases exhibit different image qualities varying in size depending on acquisition sensors, as reported in Table 1. Fingerprints are captured at different instances and some good quality images were deliberately removed to create challenges for algorithms. While capturing the fingerprints, sensors were neither cleaned nor moistness was considered to be removed [15]. Some distorted and poor quality fingerprints are shown in Figures 4a–4c.

Table 1: Description of data bases.

Sr. no.	Data base	Sensor type	Resolution (dpi)	Image size
1	FVC2000DB1A	Optical sensor	500	300 by 300
2	FVC2002DB1A	Identix TouchView II	500	388 by 374
3	FVC2006DB1A	Electric Field sensor	250	96 by 96
4	LivDet2009	Crossmatch	500	480 by 640



Figure 4: (a), (b) and (c) Poor quality images from the used databases.

### 7.2. FNMR and FMR

*FNMR* and *FMR* are two important parameters to interpret the error of a biometric system. For genuine matching, a particular finger is compared and matched with all samples and the same procedure is used for all fingers. On the contrary, for the execution of imposter matching, only the first sample of each finger is compared and *FMR* is observed. The point where *FNMR* and *FMR* become equal is called EER that depicts the overall error of the system as shown in Figures 5a–5d, where  $FNMR(t)$  and  $FMR(t)$  are plotted and value of  $t$  is provided in legend of each case.

<sup>1</sup>FVC2000 Database [online]. Website <http://bias.csr.unibo.it/fvc2000/download.asp> [accessed 15 03 2016]

<sup>2</sup>FVC2002 Database [online]. Website <http://bias.csr.unibo.it/fvc2002/download.asp> [accessed 21 07 2016]

<sup>3</sup>FVC2006 Database [online]. Website <http://bias.csr.unibo.it/fvc2006/databases.asp> [accessed 19 12 2016]

<sup>4</sup>LivDet2009 Database [online]. Website <http://livdet.org/reports.php> [accessed 26 11 2019]



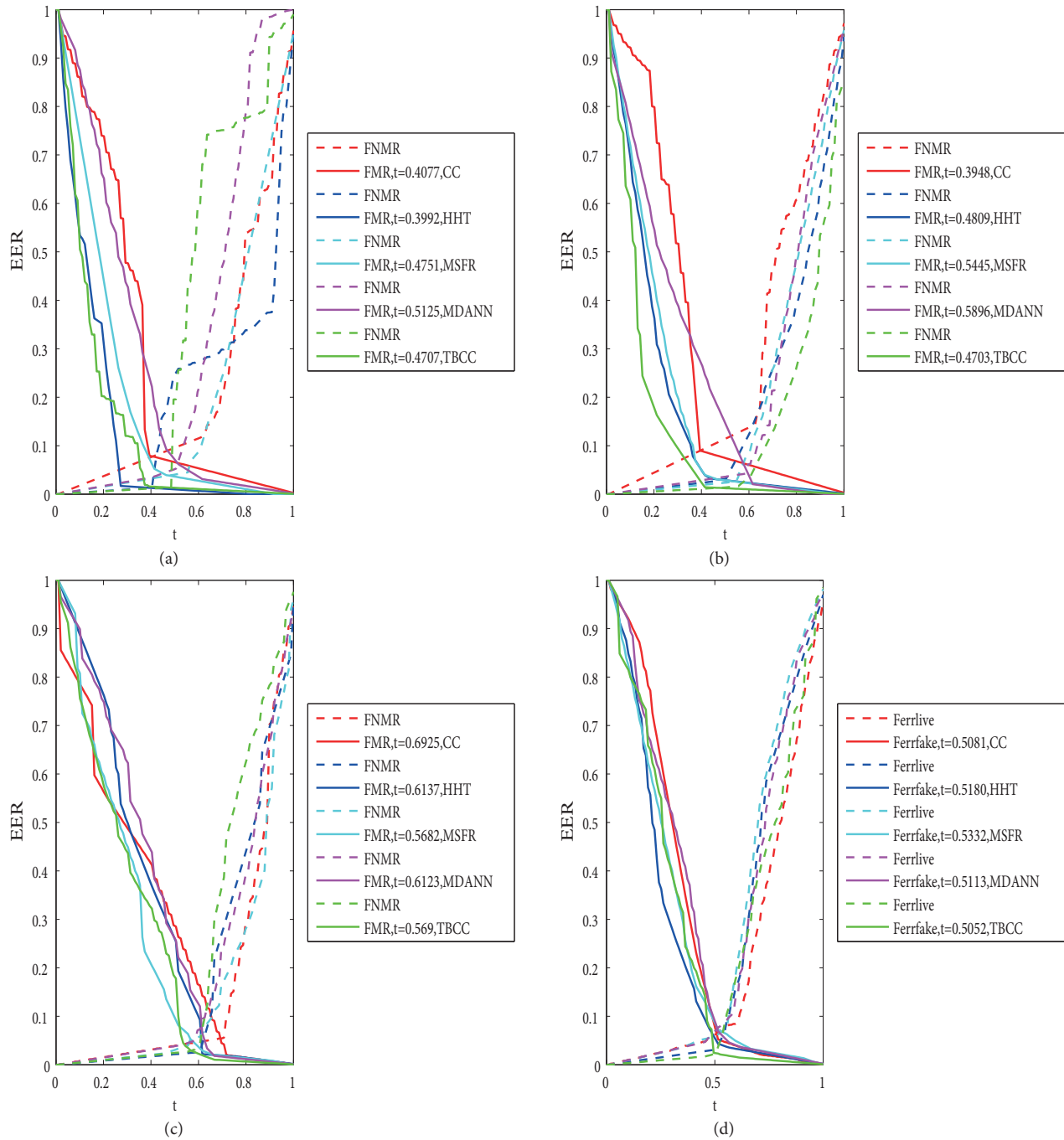


Figure 5: (a): FNMR( $t$ ) and FMR( $t$ ) curves for FVC2000DB1A, (b) FNMR( $t$ ) and FMR( $t$ ) curves for FVC2002DB1A, (c): FNMR( $t$ ) and FMR( $t$ ) curves for FVC2006DB1A, (d): Ferrlive( $t$ ) and Ferrfake( $t$ ) curves for LivDet2009 fingerprint databases.

### 7.3. Parameters

Based on outcomes of matching-scores of algorithms, different statistical parameters are employed to depict the comparison of performance in terms of  $A$  as given in Table 2.

#### 7.4. TBCC based implementation

While performing matching with TBCC, features such as minutiae points (ridge endings and ridge bifurcations) are obtained, unlike *CC*. Alignment is carried out as discussed in section 5 and correlation is performed for the extracted features instead of whole finger's ridges that reduce matching time as well as computations for ongoing images, as illustrated in Table 2 and Table 3, respectively.

Table 2: Computational time and accuracies.

Sr. no.	Algorithm	Data Base	ATFE(sec)	ATFM(sec)	A(%)
1	CC	FVC2000DB1A	3.1584	57.2959	92.42
2	HHT	FVC2000DB1A	10.3754	7.5673	96.82
3	MSFR	FVC2000DB1A	1.5583	0.5166	95.79
4	MDANN	FVC2000DB1A	4.1134	0.7881	93.71
5	TBCC	FVC2000DB1A	3.7475	0.0047	97.34
6	CC	FVC2002DB1A	3.7025	130.1576	91.5
7	HHT	FVC2002DB1A	15.5378	11.0394	96.99
8	MSFR	FVC2002DB1A	2.5126	0.8331	96.83
9	MDANN	FVC2002DB1A	5.4622	1.2528	91.96
10	TBCC	FVC2002DB1A	4.2388	0.0079	96.97
11	CC	FVC2006DB1A	0.3259	5.8699	95.03
12	HHT	FVC2006DB1A	1.0924	0.7991	96.22
13	MSFR	FVC2006DB1A	0.1595	0.0529	95.11
14	MDANN	FVC2006DB1A	0.4042	0.0789	93.15
15	TBCC	FVC2006DB1A	1.2683	0.0023	97.22
16	CC	LivDet2009	9.7106	194.41	94.2
17	HHT	LivDet2009	33.198	23.6397	95
18	MSFR	LivDet2009	5.3191	1.7636	93.19
19	MDANN	LivDet2009	12.0234	2.6784	92.85
20	TBCC	LivDet2009	5.1065	0.0095	96.49

Table 3: Computations.

Sr. no.	Data base	Algorithm	Multiplications	Additions
1	FVC2000DB1A	<i>CC</i>	90000	89999
2	FVC2002DB1A	<i>CC</i>	145112	145111
3	FVC2006DB1A	<i>CC</i>	9216	9215
4	LivDet2009	<i>CC</i>	307200	307199
5	FVC2000DB1A	TBCC	315	314
6	FVC2002DB1A	TBCC	381	380
7	FVC2006DB1A	TBCC	114	113
8	LivDet2009	TBCC	459	458

Blind rotations in *CC* bring error at those points where ridge and valley overlap while performing correlations that increases the computational cost as well as matching time. However, TBCC is independent of this constraint and relies on prior alignment according to features of the template image followed by correlation

avoiding redundant correlations. Hence, it decreases computations and executes matching in a lesser amount of time. Since, computations of TBCC-based correlations depend on  $\min(m, n)$ , therefore, it decreases numbers of correlations accordingly. Similarly, TBCC performs correlations among aligned minutiae points, therefore, the likelihood of redundant correlations decreases causing reduction in error and that's why  $FNMR$  and  $FMR$  decrease and  $A$  is increased as shown in receiver operating characteristic curve (ROC) in Figures 6a–6d, respectively. Moreover, for comparison different algorithms such as hierarchical hough transform (HHT) [22], multilevel structural technique for fingerprint recognition (MSFR) [23] and multi-dimensional artificial neural network (MDANN) [24] based algorithms are implemented and their results are illustrated in Figures 6a–6d, respectively.

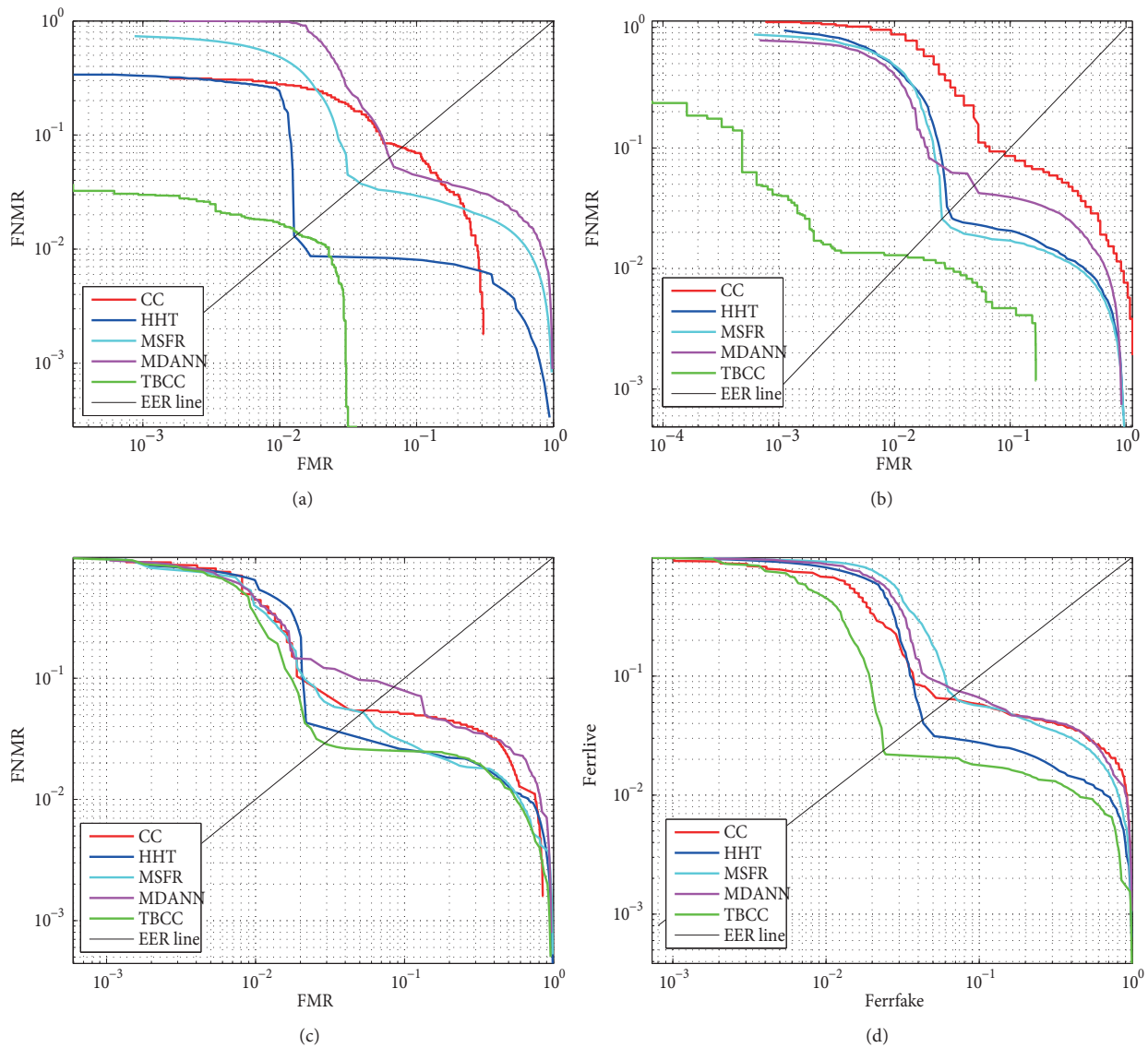


Figure 6: (a): ROC curve for FVC2000DB1A, (b) ROC curve for FVC2002DB1A, (c): ROC curve for FVC2006DB1A, (d): ROC curve for LivDet2009 fingerprint databases.

### 7.5. Enrolment time

Average time for features extraction (ATFE) and average time for features matching (ATFM) is reported in Table 2. This time is noted using a corei5 computer with 4 GB RAM and 2.7 GHz processor.

### 7.6. Computations

The computations for a single cross-correlation and its corresponding additions are exemplarily reported in Table 3 explicitly for the databases used in this paper. The number of reduced computations by TBCC can be observed.

### 7.7. Improvement in accuracy

The improvement in accuracy (IIA) is reported in Table 4 and comparison with recent methods is provided in Table 5.

Table 4: Improvement in accuracy.

Sr. no.	Data base	Algorithm	IIA (%)
1	FVC2000DB1A	TBCC	4.9162
2	FVC2002DB1A	TBCC	5.4697
3	FVC2006DB1A	TBCC	2.1878
4	LivDet2009	TBCC	2.289

Table 5: Comparison with recent methods.

Sr. no.	Method	EER (%)
1	J De Boer et al. [25]	1.34
2	Gao et al. [26]	3.5
3	Guangming et al. [27]	3.05
4	W. Chen et al. [9]	8
5	J. Feng et al. [28]	1.8
6	M. Kaur et al. [29]	2
7	R. P. Sharma et al. [30]	0.56
8	Proposed method (TBCC)	1.29

## 8. Conclusions

This paper presents a cross-correlation based technique to overcome computations of a computationally expensive matching method. The fingerprint image first undergoes through the enhancement process and then thinning is performed to extract features (minutiae points such as ridge-endings and ridge-bifurcations). The remaining parts of the ridges are discarded to avoid misalignment errors as well as to reduce computations. Orientation and  $x$ - $y$  locations of extracted features are obtained to ease alignment and then cross-correlation is performed among features of ongoing images to produce the score using different fingerprint databases. A significant amount of computations, as well as error, are reduced. The proposed technique outperforms the existing algorithms by producing better accuracy in less time.

## References

- [1] Maltoni D, Maio D, Jain AK, Prabhakar S. Handbook of fingerprint recognition. USA: Springer Science & Business Media, 2009.
- [2] Jain AK, Feng J, Nandakumar K. Fingerprint matching. *Computer* 2010; 43 (2): 36-44. doi: 10.1109/MC.2010.38
- [3] Zhang D, Liu F, Zhao Q, Lu G, Luo N. Selecting a reference high resolution for fingerprint recognition using minutiae and pores. *IEEE Transactions on Instrumentation and Measurement* 2011; 60 (3): 863-871. doi:10.1109/TIM.2010.2062610
- [4] Bae G, Lee H, Son S, Hwang D, Kim J. Secure and robust user authentication using partial fingerprint matching. In: 2018 IEEE International Conference on Consumer Electronics (ICCE). IEEE, Las Vegas, USA; 2018. p. 1-6.
- [5] Derman E, Keskinöz M. Normalized cross-correlation based global distortion correction in fingerprint image matching. In: IEEE 2016 International Conference on Systems, Signals and Image Processing (IWSSIP). Bratislava, Slovakia; 2016. p. 1-4.
- [6] Werner GA, Hanka L. Tuning an artificial neural network to increase the efficiency of a fingerprint matching algorithm. In: IEEE 2016 14th International Symposium on Applied Machine Intelligence and Informatics (SAMi). Herlany, Slovakia; 2016. p. 105-109.
- [7] Peralta D, Garc'ia S, Benitez JM, Herrera F. Minutiae-based fingerprint matching decomposition: methodology for big data frameworks. *Information Sciences* 2017; 408: 198-212. doi: 10.1016/j.ins.2017.05.001
- [8] Lee W, Cho S, Choi H, Kim J. Partial fingerprint matching using minutiae and ridge shape features for small fingerprint scanners. *Expert Systems with Applications* 2017; 87: 183-198. doi: 10.1016/j.eswa.2017.06.019
- [9] Chen W, Fan W, Xi X, Yang Z, Yang J. A novel fast fingerprint matching method based on feature descriptors. In: 2018 IEEE 3rd Advanced Information Technology, Electronic and Automation Control Conference (IAEAC). IEEE, Chongqing, China; 2018. p. 2106-2109.
- [10] Tico M, Kuosmanen P. Fingerprint matching using an orientation-based minutia descriptor. *IEEE Transactions on Pattern Analysis and Machine Intelligence* 2003; 25 (8): 1009-1014. doi: 10.1109/TPAMI.2003.1217604
- [11] Feng J. Combining minutiae descriptors for fingerprint matching. *Pattern Recognition* 2008; 41 (1): 342-352. doi: 10.1016/j.patcog.2007.04.016
- [12] Kovacs-Vajna ZM. A fingerprint verification system based on triangular matching and dynamic time warping. *IEEE Transactions on Pattern Analysis and Machine Intelligence* 2000; 22 (11): 1266-1276. doi: 10.1109/34.888711
- [13] Hong L, Wan Y, Jain A. Fingerprint image enhancement: Algorithm and performance evaluation. *IEEE Transactions on Pattern Analysis and Machine Intelligence* 1998; 20 (8): 777-789. doi: 10.1109/34.709565
- [14] Jain AK, Farrokhnia F. Unsupervised texture segmentation using Gabor filters. *Pattern Recognition* 1991; 24 (12): 1167-1186. doi: 10.1016/0031-3203(91)90143-S
- [15] Maio D, Maltoni D, Cappelli R, Wayman JL, Jain AK. FVC2002: Second fingerprint verification competition. In: Proceeding of 16th IEEE international conference on Pattern recognition, 2002. Quebec, Canada; 2002. p. 811-814.
- [16] Xiao Q, Raafat H. Fingerprint image postprocessing: a combined statistical and structural approach. *Pattern Recognition* 1991; 24 (10): 985-992. doi: 10.1016/0031-3203(91)90095-M
- [17] Cappelli R, Ferrara M, Maltoni D. Minutia cylinder-code: A new representation and matching technique for fingerprint recognition. *IEEE Transactions on Pattern Analysis and Machine Intelligence* 2010; 32 (12): 2128-2141. doi: 10.1109/TPAMI.2010.52
- [18] Maio D, Maltoni D, Cappelli R, Wayman JL, Jain AK. FVC2000: Fingerprint verification competition. *IEEE Transactions on Pattern Analysis and Machine Intelligence* 2002; (3): 402-412. doi: 10.1109/34.990140
- [19] Fawcett T. An introduction to ROC analysis. *Pattern Recognition Letters* 2006; 27 (8): 861-874. doi: 10.1016/j.patrec.2005.10.010

- [20] Cappelli R, Ferrara M, Franco A, Maltoni D. Fingerprint verification competition 2006. *Biometric Technology Today* 2007; 15 (7-8): 7-9. doi: 10.1016/S0969-4765(07)70140-6
- [21] Marcialis GL, Lewicke A, Tan B, Coli P, Grimberg D et al. First international fingerprint liveness detection competition|LivDet 2009. In: *International Conference on Image Analysis and Processing*. Springer, Berlin, Heidelberg; 2009. p. 12-23.
- [22] Liu C, Xia T, Li H. A hierarchical hough transform for fingerprint matching. In: *International Conference on Biometric Authentication*. Springer, Berlin Heidelberg; 2004. p. 373-379.
- [23] Shalaby MW, Ahmad MO. A multilevel structural technique for fingerprint representation and matching. *Signal Processing* 2013; 93 (1): 56-69. doi: 10.1016/j.sigpro.2012.06.021
- [24] Kumar R, Vikram BD. Fingerprint matching using multi-dimensional ANN. *Engineering Applications of Artificial Intelligence* 2010; 23 (2): 222-228. doi: 10.1016/j.engappai.2009.11.005
- [25] De Boer J, Bazen AM, Gerez SH. Indexing fingerprint databases based on multiple features. In: *ProRISC the 12th Annual Workshop on Circuits, Systems and Signal Processing*; Veldhoven, Netherlands; 2001. p. 300-306.
- [26] Gao Z, You X, Zhou L, Zeng W. A novel matching technique for fingerprint recognition by graphical structures. In: *2011 International Conference on Wavelet Analysis and Pattern Recognition (ICWAPR) IEEE*; Guilin, China; 2011. p. 77-82.
- [27] Lu G, Xu Y. Fast pore matching method based on deterministic annealing algorithm. *IET Image Processing* 2017; 11 (11): 1034-1040. doi: 10.1049/iet-ipr.2017.0138
- [28] Feng J, Ouyang Z, Cai A. Fingerprint matching using ridges. *Pattern Recognition* 2006; 39 (11): 2131-2140. doi: 10.1016/j.patcog.2006.05.001
- [29] Kaur M, Sofat S. Real-time chaff generation for a biometric fuzzy vault. *Turkish Journal of Electrical Engineering & Computer Sciences* 2018; 26 (1): 89-100. doi: 10.3906/elk-1610-255
- [30] Sharma RP, Dey S. Fingerprint liveness detection using local quality features. *The Visual Computer* 2019; 35 (10): 1393-1410. doi: 10.1007/s00371-018-01618-x